MOLECULAR AND CELLULAR BIOLOGY, Sept. 2001, p. 6139–6150 Vol. 21, No. 18
0270-7306/01/$04.00+0 DOI: 10.1128/MCB.21.18.6139–6150.2001

Regulation of the Yeast Yap1p Nuclear Export Signal Is Mediated by Redox Signal-Induced Reversible Disulfide Bond Formation

SHUSUKE KUGE,[1,2]* MINETARO ARITA,[1] ASAKO MURAYAMA,[1] KAZUHIRO MAETA,[3] SHINGO IZAWA,[3] YOSHIHARU INOUE,[3] AND AKIO NOMOTO[1]

Department of Microbiology, Graduate School of Medicine, The University of Tokyo, Hongo, Bunkyo-ku Tokyo 113-0033,[1] Laboratory of Molecular and Biochemical Toxicology, Graduate School of Pharmaceutical Sciences, Tohoku University, Aoba-ku, Sendai 980-8578,[2] and Laboratory of Molecular Microbiology, Division of Applied Life Sciences, Graduate School of Agriculture, Kyoto University, Uji, Kyoto 611-0011,[3] Japan

Received 22 December 2000/Returned for modification 15 February 2001/Accepted 22 June 2001

Yap1p, a crucial transcription factor in the oxidative stress response of *Saccharomyces cerevisiae*, is transported in and out of the nucleus under nonstress conditions. The nuclear export step is specifically inhibited by H_2O_2 or the thiol oxidant diamide, resulting in Yap1p nuclear accumulation and induction of transcription of its target genes. Here we provide evidence for sensing of H_2O_2 and diamide mediated by disulfide bond formation in the C-terminal cysteine-rich region (c-CRD), which contains 3 conserved cysteines and the nuclear export signal (NES). The H_2O_2 or diamide-induced oxidation of the c-CRD in vivo correlates with induced Yap1p nuclear localization. Both were initiated within 1 min of application of oxidative stress, before the intracellular redox status of thioredoxin and glutathione was affected. The cysteine residues in the middle region of Yap1p (n-CRD) are required for prolonged nuclear localization of Yap1p in response to H_2O_2 and are thus also required for maximum transcriptional activity. Using mass spectrometry analysis, the H_2O_2-induced oxidation of the c-CRD in vitro was detected as an intramolecular disulfide linkage between the first (Cys^{598}) and second (Cys^{620}) cysteine residues; this linkage could be reduced by thioredoxin. In contrast, diamide induced each pair of disulfide linkage in the c-CRD, but in this case the cysteine residues in the n-CRD appeared to be dispensable for the response. Our data provide evidence for molecular mechanisms of redox signal sensing through the thiol-disulfide redox cycle coupled with the thioredoxin system in the Yap1p NES.

All organisms growing in the presence of oxygen must continuously combat exposure to oxidative toxicity caused by reactive oxygen species (ROS), which are known to be produced by the process of reduction of molecular oxygen. In the process of respiration or oxidation of nutrients, some enzymes produce superoxide anions ($O_2^{\cdot -}$), which can be converted to H_2O_2 by superoxide dismutase. Highly reactive hydroxyl radicals (OH^-), produced from H_2O_2 in the presence of metal ions, can damage cellular components, including proteins, lipids, and DNA (10). ROS can also be produced in cells exposed to environmental stress caused by heavy metals, ionizing radiation, and redox-recycling chemicals, all of which affect the cellular thiol-disulfide balance (redox status). Not surprisingly, therefore, organisms constitutively exposed to such environmental conditions have evolved a cellular defense system that helps them maintain a suitable redox status. The first step of this defense system is the perception of redox signals caused by ROS. The signal is then transmitted to specific transcription factor(s), leading to transcriptional activation of genes that encode antioxidant enzymes and molecules. It has been proposed that this redox status is maintained by the tripeptide glutathione (GSH) (20), a major thiol in cells, and by the reducing activity of thioredoxin (28), where both systems require NADPH as an electron donor. Hence, this model suggests that the mechanisms of redox sensing are coupled to the cellular redox status (2).

In *Escherichia coli*, there exist two specialized defense systems: one system includes those genes that are regulated by the OxyR transcription factor in response to H_2O_2, while the other system includes those genes that are regulated by SoxR in response to superoxide (34). Interestingly, OxyR activity is regulated by reversible disulfide bond formation coupled with the glutaredoxin-glutathione (Grx-GSH/GSSG) system as a hydrogen donor (33). This is a prokaryotic example of the sensor for redox signaling.

Recent studies of the budding yeast *Saccharomyces cerevisiae* have indicated that the Yap1p (yeast AP-1; formerly named yAP-1) transcription factor is responsible for regulating the genes that encode cellular enzymatic or nonenzymatic processes for the oxidative stress defense system (3, 15, 29). Yap1p is a bZIP-containing factor that has homology within its DNA-binding domain to members of the mammalian Jun family of proteins (22). Disruption of the *YAP1* gene resulted in a significant increase in sensitivity to oxidative stress by hydrogen peroxide (H_2O_2, *t*-butyl hydrogen peroxide) and thiol oxidants (diamide and diethyl maleate) (17) and to cadmium toxicity (30). Yap1p can control multiple target genes that can elevate reduced glutathione and thioredoxin levels, both of which are essential for the response to oxidative stress (3, 15). Interestingly, genetic experiments indicate that thioredoxin, but not glutaredoxin, functions as a negative regulator of Yap1p nuclear localization and transcriptional activation (13), suggesting that thioredoxin-coupled redox regulation controls Yap1p nuclear localization.

* Corresponding author. Mailing address: Laboratory of Molecular and Biochemical Toxicology, Graduate School of Pharmaceutical Sciences, Tohoku University, Aza-aoba, Aramaki, Aoba-ku, Sendai, Miyagi 980-8578, Japan. Phone: 81-22-217-6872. Fax: 81-22-217-6872. E-mail: skuge@mail.pharm.tohoku.ac.jp.

It has been shown previously that Yap1p activity is controlled primarily at the level of nuclear localization (18). Yap1p is constitutively transported in and out of the nucleus, so that the concentration of Yap1p in the nucleus is relatively low under nonstress conditions. However, when oxidative stress is imposed, the nuclear export step is inhibited specifically due to the dissociation of Yap1p from the export receptor Crm1p/Xpo1p, resulting in localization of Yap1p to the nucleus (19, 32). The C-terminal cysteine-rich domain (c-CRD) of Yap1p, which contains the nuclear export signal (NES), is responsible for this regulated interaction with Crm1p. A model in which oxidation of the cysteine residues in the c-CRD changes the conformation and thus inhibits Yap1p-Crm1p interaction by concealing the NES has been proposed, based on the observation that 3 cysteine residues in the c-CRD are essential for the oxidative stress-induced nuclear localization (18), as well as the oxidative stress-induced inhibition, of the Crm1p-Yap1p interaction (19, 32).

It has been shown previously that the c-CRD alone can confer regulation of nuclear export by diamide when fused to the Gal4p DNA-binding domain (Gal4db) with green fluorescent protein (GFP) (18), indicating that the c-CRD can function as an oxidation-sensitive NES (Fig. 1A). However, a requirement for the middle cysteine-rich region (n-CRD) has also been identified for the H_2O_2-induced activation of Yap1p-target genes, including *TRX2* encoding thioredoxin, and thus for H_2O_2 tolerance (6). Therefore, the H_2O_2-induced activation of Yap1p is different from that of diamide. Recently, Delaunay et al. (7) have shown that oxidation of Yap1p, detected as a mobility shift in sodium dodecyl sulfate-polyacrylamide gel electrophoresis (SDS-PAGE), is induced specifically by H_2O_2. Their results indicate that 2 cysteine residues, 1 in the n-CRD (Cys^{303}) and 1 in the c-CRD (Cys^{598}), are essential for this oxidation; these cysteines are proposed to form disulfide bonds, which can then be reduced by thioredoxin. However, the molecular mechanism of the oxidation processes to conceal NES and the roles of other cysteine residues involved in the stress response have not been elucidated. Furthermore, the fact that diamide does not change the mobility of Yap1p (7) suggests that oxidant-specific oxidation processes are carried out.

Here we provide evidence for the sensing of H_2O_2 and diamide through reversible disulfide linkage between cysteine residues in the c-CRD of Yap1p. Our data suggest mechanisms by which how Yap1p can sense these oxidants before cellular redox status is affected.

MATERIALS AND METHODS

Yeast strains and media. Yeast cells were grown in a synthetic dextrose (SD) medium supplemented with amino acids (SD dropout) (8). Cells were subjected to oxidative stress by the addition of diamide (Sigma) or H_2O_2 as previously described (18). To generate yeast strains containing a *trx2-lacZ* reporter gene, a *Ban*II-*Bam*HI fragment containing *trx2-lacZ* was isolated from plasmid TRX-LACZ (17) and inserted in the *Stu*I site of the *URA3* gene in plasmid pUC-URA3 (17), and W303B was transformed with the DNA fragment obtained by cutting with *Hin*dIII. The *YAP1* gene was then disrupted by transfection with *yap1*::*URA3* DNA as described earlier (17). The genotypes of the strains are as follows: TY (*MAT*α *his3 can1 ade2 leu2 trp1 ura3*::*trx2-lacZ*) and TW (*MAT*α *his3 can1 ade2 leu2 trp1 ura3*::*trx2-lacZ yap1*::*URA3*). A thioredoxin-deficient strain derived from W303 was constructed as described (13). The genotype of the resulting strain *trx1*Δ *trx2*Δ is *MAT*α *his3 can1 ade2 leu2 trp1 trx1*::*URA3 trx2*::*LEU2*.

Plasmid construction. Plasmids used for expression of Yap1p in this study are listed in Table 1. All the GFP-Yap1p-expressing plasmids (pRS cp-GFP HA) used were constructed based on pRS cp-GFP HA YAP1 (17). To construct pRS cp-GFP HA yap1 3Cys, mutations of C303T, C310T, and C315T were introduced by a two-step PCR procedure as described earlier (18). PCR a was carried out using pUC-YAP1–3 (15) as a template with primers 3Cys (+), 5′-GTT TCG GAG TTT *AC*T TCG AAA ATG AAC CAG GTA *ACA* GGA ACA AGG CAA *AC*T CCC ATT CCC AAG-3′, and YAP1 C-term, 5′-GGCGAAAAGGCGAA GCAAGGT-3′ (substituted nucleotides are italicized). Reaction b was carried out using primers YAP1–1042, 5′-AGTGACGCTACAGATTCCTCC-3′, and Cys303 (−), 5′-TTT CGA A*GT* AAA CTC CGA AAC TTG TTC 3′. The products of PCRs a and b, which have overlapping sequences, were purified and subjected to the second PCR without primers. The resulting fragment was digested with *Nde*I and *Bst*XI and cloned into pUC-YAP1–3, and then a 732-bp *Bst*XI-AflIII fragment from the resulting plasmid was cloned into pRS cp-GFP HA YAP1. To generate the bacterial expression plasmid pGEX-GFP-c-CRD, both the *Eco*RV-*Mun*I fragment containing *GFP536* (27) and the *Mun*I-*Sal*I fragment containing *c-CRD* isolated from pAS1-GFP-CRD (19) were ligated between the blunt-ended *Eco*RI site and the *Sal*I site of the pGEX-6P-2 (Amersham Pharmacia). To construct pGEX-ΔGFP-c-CRD, the *GFP* region of pGEX-GFP-c-CRD was deleted by self-ligation of blunt-ended *Bam*HI and *Mun*I sites. To construct pRS GFP-c-CRD, first pRS cp-HA B-S was generated from pRS cp-GFP HA YAP1 by deleting *GFP* and *YAP1* sequences and inserting the *ADH1* terminator as described earlier (19). The coding sequence of the hemagglutinin (HA) tag region of this vector is as follows: truncated constitutive *CUP1* promoter, 5′-CTGCAG GAATTC CCCT GCC ATG TAC CCA TAC GAT GTT CCA GAT TAC GCT GGATCC GTCGAC CTGCAG CCAAGC TAA-3′, (*ADH1* terminator. Then the *Bam*HI-SalI fragment containing *GFP-c-CRD* isolated from pGEX-GFP-c-CRD was introduced between *Bam*HI and *Sal*I of pRS cp-HA B-S. A *c-CRD* mutant segment [c-$CRD^{(TAT)}$] in which all cysteine residues were mutated (C598T, C620A, and C629T) was introduced into pRS GFP-c-CRD as follows: an *Nco*I-*Sal*I fragment containing a *c-*$CRD^{(TAT)}$ region and a *Mun*I-*Bsp*HI fragment of *GFP536* were isolated from the PCR using pRS cp-GFP HA yap1 cm46A5 and *GFP536* for templates, respectively, as described earlier (18), and were introduced between the *Mun*I and *Sal*I sites of pRS GFP-c-CRD.

Confocal laser scanning microscopy and Western blotting. Confocal laser scanning microscopy and Western blotting analysis were carried out as previously described (18). Yeast cell lysates were separated by SDS-PAGE in Tris-glycine

FIG. 1. Disulfide bond formation in the Yap1p c-CRD. (A) Importance of domains and the cysteine residues of Yap1p for the induction of nuclear localization. Schematic representations of Yap1p ($Yap1p^{WT}$) and its derivatives are shown. The leucine zipper domain (ZIP; amino acid positions 71 to 121), the n-CRD (position undefined as a domain), and the c-CRD (amino acid positions 577 to 650) are indicated together with the positions of 6 cysteine (C) residues. A mutant with all 3 c-CRD cysteines replaced [$Yap1p^{(TAT)}$, with C598T, C620A, and C629T mutations] and the fusion construct of c-CRD fused to Gal4db and GFP (GAL4db-GFP-c-CRD) is shown. Previously observed (18) phenotypes are indicated. The GFP-c-CRD and ΔGFP-c-CRD used for this study are also shown. (B) TW (*yap1*) cells carrying pRS HA GFP-c-CRD were untreated (cont) or treated with 0.5 mM H_2O_2 or 1.5 mM diamide for 30 min. Free thiols were blocked by IAA and were further analyzed for molecular-weight shift by nonreducing SDS-PAGE as described in Materials and Methods. Positions of molecular-weight markers are shown. (C) Lysyl endopeptidase sites (amino acid numbers of lysine residues are indicated) in the c-CRD. The peptides CP1, CP2, and CP3, together with these molecular masses, corresponding to the peptide fragments containing Cys^{598}, Cys^{620}, and Cys^{629} are shown. (D) Peptide analysis of the c-CRD. The ΔGFP-c-CRD was incubated with 1 mM H_2O_2 (lanes 3, 5, and 7) or 2 mM diamide (lanes 2, 4, and 6) or no oxidant (lane 1) and was analyzed for lysyl endopeptidase-digested peptide fragments as described in Materials and Methods. IAA treatment was carried out before oxidation (lane 2 and 3) or after oxidation (lanes 4 and 5) or after the peptidase digestion (lanes 6 and 7). (E to G) MALDI-TOF spectra for reduced (E), 1 mM H_2O_2-treated (F), and 2 mM diamide-treated (G) GFP-c-CRD after lysyl endopeptidase digestion. The peptide peaks CP1, CP2, and CP3 are shown (E). The peaks corresponding to CP1 linked to CP2 (CP1–2) (F and G), CP1 linked to CP3 (CP1–3) (G), and CP2 linked to CP3 (CP2–3) (G) are indicated.

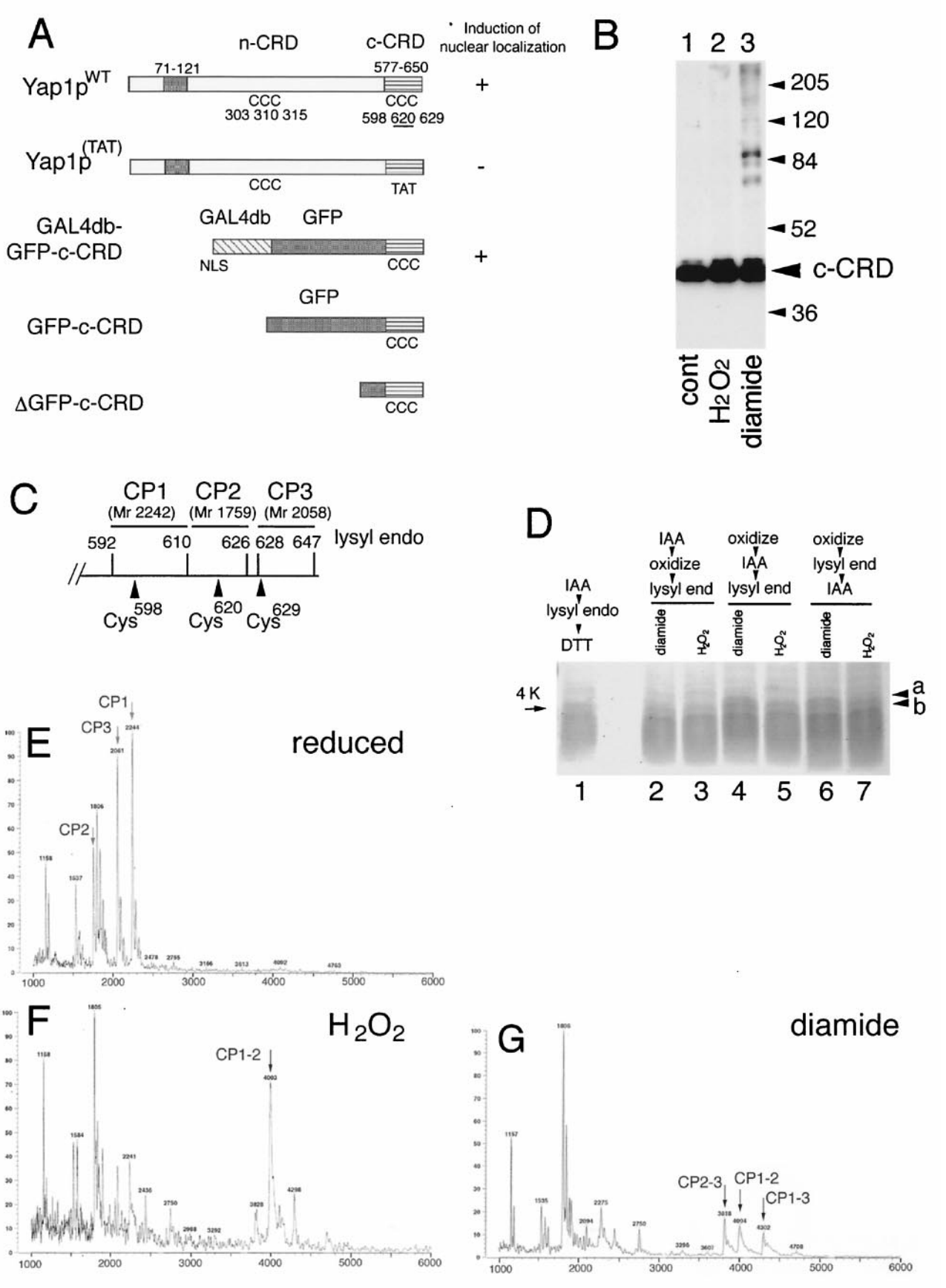
A
n-CRD
c-CRD
* Induction of nuclear localization
Yap1p^WT
71-121
577-650
CCC 303 310 315
CCC 598 620 629
+
Yap1p^(TAT)
CCC
TAT
-
GAL4db-GFP-c-CRD
GAL4db
GFP
NLS
CCC
+
GFP-c-CRD
GFP
CCC
ΔGFP-c-CRD
CCC
B
1 2 3
205
120
84
52
c-CRD
36
cont
H2O2
diamide
C
CP1 (Mr 2242)
CP2 (Mr 1759)
CP3 (Mr 2058)
592 610 626 628 647
lysyl endo
Cys598 Cys620 Cys629
D
IAA
lysyl endo
DTT
IAA
oxidize
lysyl end
oxidize
IAA
lysyl end
oxidize
lysyl end
IAA
diamide
H2O2
4 K
a
b
1 2 3 4 5 6 7
E
reduced
CP1
CP3
CP2
F
H2O2
CP1-2
G
diamide
CP2-3
CP1-2
CP1-3

TABLE 1. Expression plasmids used in this study

Plasmid (purposes)	Expressing protein	Reference
Yeast Yap1p expression plasmids (localization and activity)		
pRS cp-GFP HA YAP1	GFP-fused Yap1pWT	18
pRS cp-GFP HA yap1 C598T	GFP-fused Yap1p^{C598T}	18
pRS cp-GFP HA yap1 C620A	GFP-fused Yap1p^{C620A}	18
pRS cp-GFP HA yap1 C629T	GFP-fused Yap1p^{C629T}	18
pRS cp-GFP HA yap1 cm46A5	GFP-fused Yap1p$^{(TAT)}$ (C598T, C620A, C629T)	18
pRS cp-GFP HA yap1 3Cys	GFP-fused Yap1p^{3Cys} (C303T, C310T, C315T)	This study
pRS cp-GFP HA yap1 3Cys, C620A	GFP-fused Yap1p$^{3Cys,\ C620A}$ (C303T, C310T, C315T, C620A)	This study
Yeast c-CRD expression plasmids (oxidation process in vivo)		
pRS GFP-CRD	HA-GFP-fused c-CRD	This study
pRS GFP-CRD$^{(TAT)}$	HA-GFP-fused c-CRD$^{(TAT)}$ (C598T, C620A, C629T)	This study
Recombinant protein expression plasmids		
pGEX GFP-CRD	Recombinant c-CRD (mass spectroscopy)	This study
pGEX ΔGFP-CRD	Recombinant c-CRD (peptide assay and reduction assay)	This study

buffer (25) or by SDS–16.5% Tris-Tricine PAGE (26), transferred to polyvinyl difluoride membranes (Immobilon; Millipore), and immunoblotted using anti-HA rat monoclonal antibody (high affinity; Roche) or anti-Trx2p rabbit antibody (13), reacted with peroxidase-conjugated second antibodies (Dako), and detected using enhanced chemiluminescence and enhanced chemiluminescence hyperfilm (Amersham Pharmacia).

Protein expression and analysis. To express recombinant c-CRD proteins, exponentially growing *E. coli* cells carrying pGEX-GFP-c-CRD or pGEX-ΔGFP-c-CRD were treated with 0.5 mM isopropyl β-D-galactopyranoside (IPTG) for 3 h at 37°C. The recombinant c-CRD proteins were purified on a glutathione-Sepharose column in combination with PreSession protease as recommended by the manufacturer (Amersham Pharmacia). His-tagged Trx2p expression was carried out as described earlier (13). Purified recombinant proteins were desalted using VIVA SPIN (VIVA Science) to 10 mM Tris-HCl (pH 7.4) and were then stored at −80°C. For technical reasons, GFP-c-CRD (M_r, 36,000) was used for mass spectrometry (MS), and ΔGFP-c-CRD (M_r, 14,400), in which most of the GFP region was deleted, was used for peptide analysis and thioredoxin-dependent reduction experiments.

Peptide analysis and mass spectroscopy. Five micrograms of the recombinant c-CRD (ΔGFP-c-CRD) was incubated with 1 mM H_2O_2 or 2 mM diamide for 20 min at 30°C, digested by lysyl endopeptidase (Sigma) at 37°C for 2 h, and then separated by SDS–16.5% Tris-Tricine PAGE. A portion (2.8 μg) of the recombinant c-CRD (GFP-c-CRD) fusion proteins was oxidized and digested as described above and was then analyzed by mass spectroscopy (KOMPACT MALDI III plus; Shimadzu/Kratos) using a matrix solution containing 1% 2,5-dihydroxybenzoic acid, 0.1% 5-methoxysalicylic acid, 10% acetonitrile, and 0.1% trifluoroacetic acid.

Reduction of oxidized c-CRD by thioredoxin and in vitro detection of free thiols. All buffers and water for the reagents were degassed, and the reaction was carried out under nitrogen gas. The amounts of proteins were estimated by absorbance at 280 nm (factor of 1 A_{280} = 1.429 μg). Affinity-purified recombinant c-CRDs and His-Trx2p were further purified using the SMART system on a miniQ column (Amersham Pharmacia) after first digesting the His-Trx2p with thrombin protease (Amersham Pharmacia) to remove the His tag. Proteins (30 μg) in the peak fractions were treated with 5 mM dithiothreitol (DTT) for 30 min at room temperature, and DTT was removed through a fast-desalting column (Amersham Pharmacia) in 10 mM Tris-HCl (pH 7.5)–1 mM EDTA (TE). Then 6 μg of the reduced recombinant c-CRD (ΔGFP-c-CRD) protein was treated with diamide (2 mM) or H_2O_2 (0.2 mM or 1.0 mM) in 50 μl of TE for 30 min at room temperature and was purified by the fast-desalting column. The reduced Trx2p (0.25 μg) was reacted with an approximately equal amount (estimated by Coomassie stain) of the oxidized recombinant c-CRD in 8 μl of TE at room temperature for 30 min. After the addition of 2.5 μl of 50 mM 4-acetamido-4′-maleimidylstilbene-2,2′-disulfonic acid (AMS; Molecular Probes) in TE, further reaction was carried out at 30°C for 30 min, after which SDS was added to a concentration of 0.5% and incubation was continued at 37°C for 10 min. After the addition of 5 μl of 4× sample buffer (200 mM Tris-HCl, pH 6.8, 8% SDS, 40% glycerol, and 0.4% bromophenol blue), samples were subjected to SDS–15% PAGE (12 by 12 cm). Gels were stained with Coomassie brilliant blue R-250.

In vivo detection of disulfide by IAA/AMS assay. Yeast cells of strain TW carrying pRS GFP-c-CRD were cultured in SD dropout-Trp-Ura medium until exponential phase, and oxidative stress was imposed as indicated. To detect thiols in vivo, a combination of iodoacetamide (IAA) and AMS was used, based on the method described earlier (14). At the indicated time, IAA was added to the cultures at a final concentration of 100 mM. After 2 min of incubation, cells were fixed in 10% trichloroacetic acid on ice for 30 min. The cells were then washed five times with 10% trichloroacetic acid and then with TE (100:10) (100 mM Tris-HCl, pH 9.5, and 10 mM EDTA). The cells were then disrupted with glass beads in TE (100:10) containing 10 mM DTT and were solubilized with 0.5% SDS. Protein concentrations were determined by Bradford assay (Bio-Rad). Thirty micrograms of protein in 10 μl of TE (100:10)–10 mM DTT was incubated for 1 h at 44°C and was then incubated with 10 μl of 50 mM AMS (in TE) at 30°C for 30 min and at 37°C for 15 min. After the addition of 10 μl of 4× SDS sample buffer, half of the sample was subjected to SDS–10% PAGE (12 by 8 cm or 15 by 13 cm) for detection of HA-GFP-c-CRD and the other half was subjected to 16.5% Tris-Tricine PAGE (12 by 8 cm) for detection of thioredoxin. To analyze the possibility of molecular weight shift by intermolecular disulfide linkage with other molecules, lysate was prepared without DTT and separated with SDS–10% PAGE.

Determination of glutathione. Cells were cultured in a 200-ml flask containing 50 ml of SD medium at 30°C to an optical density at 610 nm of 0.5 and were treated with 0.5 mM H_2O_2, 0.5 mM diamide, or 1.5 mM diamide for the indicated times at 30°C. Cells were harvested by centrifugation, washed once with 0.85% NaCl solution, and suspended in 300 μl of ice-chilled 8 mM HCl solution. An approximately equal amount of glass beads was added, and cells were disrupted with a vortex mixer at the maximum speed for 2.5 min. Cell homogenates were centrifuged at 12,000 × *g* for 10 min at 4°C to obtain clear supernatants. Determination of glutathione was then done essentially as described (1). Briefly, to measure total glutathione, 20 μl of 13% sulfosalicylic acid solution in 8 mM HCl was added to 180 μl of clear supernatant; the mixture was kept on ice for 15 min and was then centrifuged at 12,000 × *g* for 10 min at 4°C. The total glutathione in the supernatant was then measured by the 5,5′-dithiobis(2-nitrobenzoic acid) (DTNB)-glutathione reductase coupling method. To measure oxidized glutathione (GSSG), 5 μl of 2-vinylpyridine was added to the clear supernatants and the mixture was kept at 28°C for 1 h. The mixture was then centrifuged at 12,000 × *g* for 10 min at 25°C. The GSSG in the supernatant was then determined by the DTNB-glutathione reductase coupling method.

RESULTS

Disulfide bond formation between c-CRD cysteine residues in vitro. To characterize the oxidation process of the cysteine residues in the Yap1p c-CRD, we first determined whether the cysteine residues in the c-CRD could form disulfide linkage with other proteins. We found that the c-CRD could be expressed stably in yeast cells only when fused with GFP. Cell lysates were prepared after free thiol groups in the live yeast

cells were blocked by the thiol-specific alkylating reagent IAA and were separated by SDS-PAGE under nonreducing condition. The c-CRD was then detected as described in Materials and Methods. As shown in Fig. 1B, no higher-molecular-weight band was observed upon oxidative stress by H_2O_2 (Fig. 1B, lane 2) and the majority of the c-CRD was detected at the same mobility as the control upon oxidative stress by diamide (Fig. 1B, lanes 1 and 3), suggesting that disulfide linkage between the c-CRD and another protein is not crucial for the Yap1p regulation.

We then pursued the possibility that intramolecular disulfide linkages might be formed in c-CRD. It has been shown that a bacterially expressed Yap1p can bind to Crm1p under reducing conditions (32), indicating that the c-CRD might not require posttranslational modification for association with Crm1p. Thus, we analyzed recombinant c-CRD proteins that could be stably expressed in *E. coli* and purified to homogeneity as described in Materials and Methods. In order to detect the three-disulfide linkage between the 3 cysteines of the c-CRD as a molecular-weight shift, the recombinant c-CRD was digested with a lysine-specific peptidase, which could separate the 3 cysteine residues into three different peptide fragments (CP1, CP2, and CP3 containing Cys^{598}, Cys^{620}, and Cys^{629}, respectively) (Fig. 1C), and was analyzed by SDS-PAGE. As shown in Fig. 1D, a peptide band, not seen in the untreated control sample, was generated when the c-CRD was treated with H_2O_2; its molecular weight was approximately 4,000 (Fig. 1D, lane 5; indicated as "b"). In addition to "b," a larger peptide band (indicated as "a") was formed when the recombinant c-CRD was treated with diamide (Fig. 1D, lane 4). These molecular-weight shifts were blocked by pretreatment of IAA (Fig. 1D, lanes 2 and 3), and the shift disappeared under DTT-containing reducing conditions (data not shown), suggesting that disulfide linkages are responsible for the molecular-weight shift of the peptides. There were no differences in the peptide patterns in the SDS-PAGE whether IAA treatment was carried out before and after the peptidase digestion (compare lanes 4 and 5 to lanes 6 and 7 in Fig. 1D), suggesting that the oxidation of the cysteine residues of the recombinant c-CRD in these experiments was completed before peptidase digestion.

To identify which cysteine residues were responsible for the molecular weight shift, matrix-assisted laser desorption ionization–time-of-flight (MS) (MALDI-TOF [MS]) was used. As shown in Fig. 1E, peptides with predicted molecular weights of 2,242 (CP1), 1,759 (CP2), and 2,058 (CP3) could be observed under reducing conditions. Next, MS analyses were carried out to detect modification by oxidation with H_2O_2 or diamide. As shown in Fig. 1F, when the c-CRD was treated with H_2O_2, CP1, CP2, and CP3 disappeared almost completely, whereas higher-molecular-weight peaks were observed. One peptide fragment (CP1–2) with a molecular weight of 4,003 corresponded to that predicted for CP1 linked to CP2 (3,999). This peak disappeared when the reaction mixture was reduced by DTT prior to MS analysis (data not shown), indicating that the linkage between CP1 and CP2 was by a disulfide linkage between Cys^{598} and Cys^{620}. In contrast, diamide induces disulfide linkages between CP1 and CP2 (Cys^{598}-Cys^{620}), CP2 and CP3 (Cys^{620}-Cys^{629}), and CP1 and CP3 (Cys^{598}-Cys^{629}) (Fig. 1G).

Cys^{598} requirement for Yap1p response to H_2O_2. To examine the importance of each of the cysteines, we investigated the effect of amino acid substitutions at the cysteine residues of Yap1p c-CRD on H_2O_2-induced *trx2-lacZ* reporter gene activation and on the nuclear localization of Yap1p. We have previously shown that $Yap1p^{C598T}$, $Yap1p^{C620A}$, and $Yap1p^{C629T}$ can respond to diamide; that is, nuclear localization and the reporter gene activation were induced (18). Interestingly, the H_2O_2-induced activation was completely inhibited when a C598T substitution (GFP-$Yap1p^{C598T}$), C629T substitution (GFP-$Yap1p^{C629T}$), or a substitution at all 3 residues [GFP-$Yap1p^{(TAT)}$] was introduced, whereas H_2O_2 could still induce the activity of GFP-$Yap1p^{C620A}$ (Fig. 2A). Consistent with these results, H_2O_2-induced nuclear localization was inhibited by C598T, C629T, or the 3-residue substitution during the course of oxidative stress, 1 to 60 min (data not shown). In addition, stronger H_2O_2 stresses (2 and 3 mM) also failed to induce the nuclear localization of $Yap1p^{C598T}$ (data not shown). Thus, we next tested the effect of an oxidizing environment in thioredoxin-deficient cells (*trx1*Δ *trx2*Δ). As previously observed with $Yap1p^{WT}$ (13), $Yap1p^{C620A}$ and $Yap1p^{C629T}$ were localized in the nucleus. However, $Yap1p^{C598T}$ and $Yap1p^{(TAT)}$ was still in the cytoplasm (Fig. 2B). Interestingly, upon oxidative stresses by H_2O_2 (0.5 and 1.0 mM) or diamide (1.5 mM), the nuclear localization of $Yap1p^{C598T}$ was induced in *trx1*Δ *trx2*Δ cells but not that of $Yap1p^{(TAT)}$ (Fig. 2C). These results support the idea that Cys^{598} is required for maximum sensitivity of Yap1p to H_2O_2.

Correlation between oxidation of c-CRD cysteine residues in vivo and induced nuclear localization. We next examined the oxidation state of the c-CRD cysteines in vivo using combination of IAA and the thiol-reactive probe AMS (molecular weight, 536) as described in Materials and Methods. In this experiment, free thiols (reduced cysteines) were first alkylated by direct addition of IAA in the culture to prevent artificial oxidation during preparation of the yeast lysates and to observe preexisting disulfide bonds by molecular-weight shift by AMS. To observe small molecular-weight changes in the c-CRD, HA-GFP-c-CRD expressing cells were used. In a control assay, we detected a higher-molecular-weight band when the cells were not treated with IAA; in this case all cysteines reacted with AMS to produce a molecular-weight shift (Fig. 3A, lane 1). In contrast, the mobility of the 3-cysteine substitution mutant c-$CRD^{(TAT)}$ was not affected by the treatment with IAA (Fig. 3A, compare lanes 3 and 4) indicating that the molecular-weight difference evident between the subjects of lanes 1 and 3 was caused by AMS modification of cysteine thiols in the c-CRD. Compared with the c-$CRD^{(TAT)}$, the c-CRD showed a broader band (Fig. 3A, compare lanes 2 and 3), suggesting that the cysteines in the c-CRD were partially oxidized under unstressed normal conditions.

We then examined the effect of oxidative stress on oxidation of the cysteine residues of the c-CRD in vivo. Interestingly, the cysteine residues in the c-CRD became oxidized 1 min after the treatment with H_2O_2 (Fig. 3B, compare lanes 1 and 2, +AMS); however, it became reduced within 5 min and stayed reduced for 30 min (Fig. 3B, compare lanes 2 and 3 to 5 of +AMS). In the case of diamide treatment, the c-CRD was oxidized at 1 min (Fig. 3B, lane 8 of +AMS) and was continuously oxidized for 30 min (Fig. 3B, lanes 8 to 11). The molecular-weight shift by H_2O_2 was smaller than that of the complete oxidized control (Fig. 3B, compare lanes 2 and 6 of

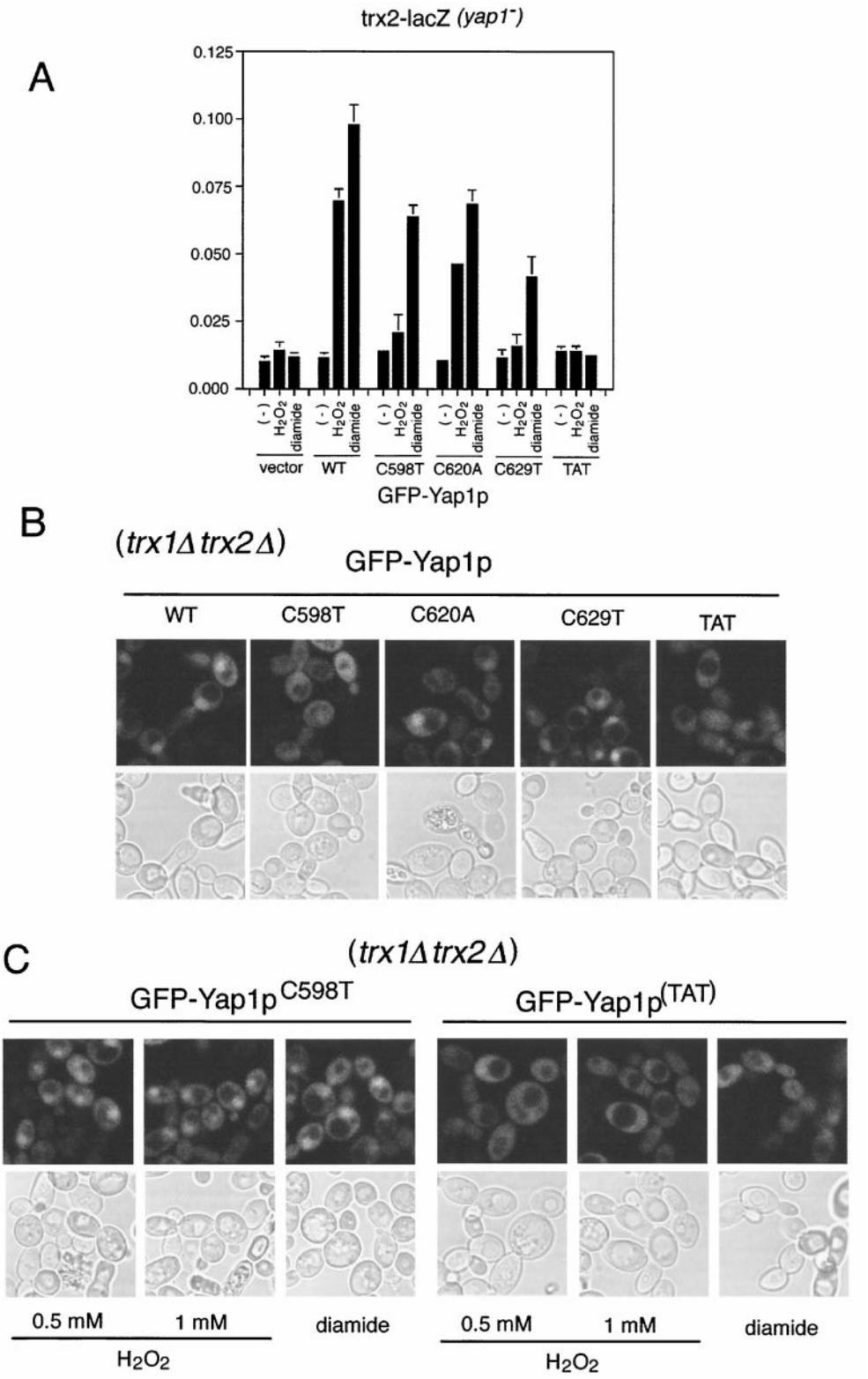

FIG. 2. Requirement for the cysteine residues in the c-CRD for the response to H_2O_2. (A) Strain TW (*yap1 trx2-lacZ*) cells expressing GFP-fused $Yap1p^{WT}$, $Yap1p^{C598T}$, $Yap1p^{C620A}$, $Yap1p^{C629T}$, or $Yap1p^{(TAT)}$ were not treated (−) or were treated with H_2O_2 (0.5 mM) or diamide (1.5 mM) for 60 min, and the reporter gene (*trx2-lacZ*) activation was observed by β-galactosidase assay as described previously (18). The averages and standard errors of triplicate samples are indicated. (B) Inhibition of the constitutive nuclear localization of Yap1p in *trx1*Δ *trx2*Δ cells by C598T substitution. The *trx1*Δ *trx2*Δ cells expressing GFP-fused $Yap1p^{WT}$, $Yap1p^{C598T}$, $Yap1p^{C620A}$, $Yap1p^{C629T}$, or $Yap1p^{(TAT)}$ were observed by confocal microscopy. (C) Nuclear localization of $Yap1p^{C598T}$ in *trx1*Δ *trx2*Δ cells treated with H_2O_2 or diamide. Cells expressing GFP-$Yap1p^{C598T}$ were grown for 30 min without stress (−) or with a stress of 0.5 mM H_2O_2, 1.0 mM H_2O_2, or 2 mM diamide and were examined by confocal microscopy. In panels B and C, both fluorescence (upper rows) and transmission (lower rows) images are shown.

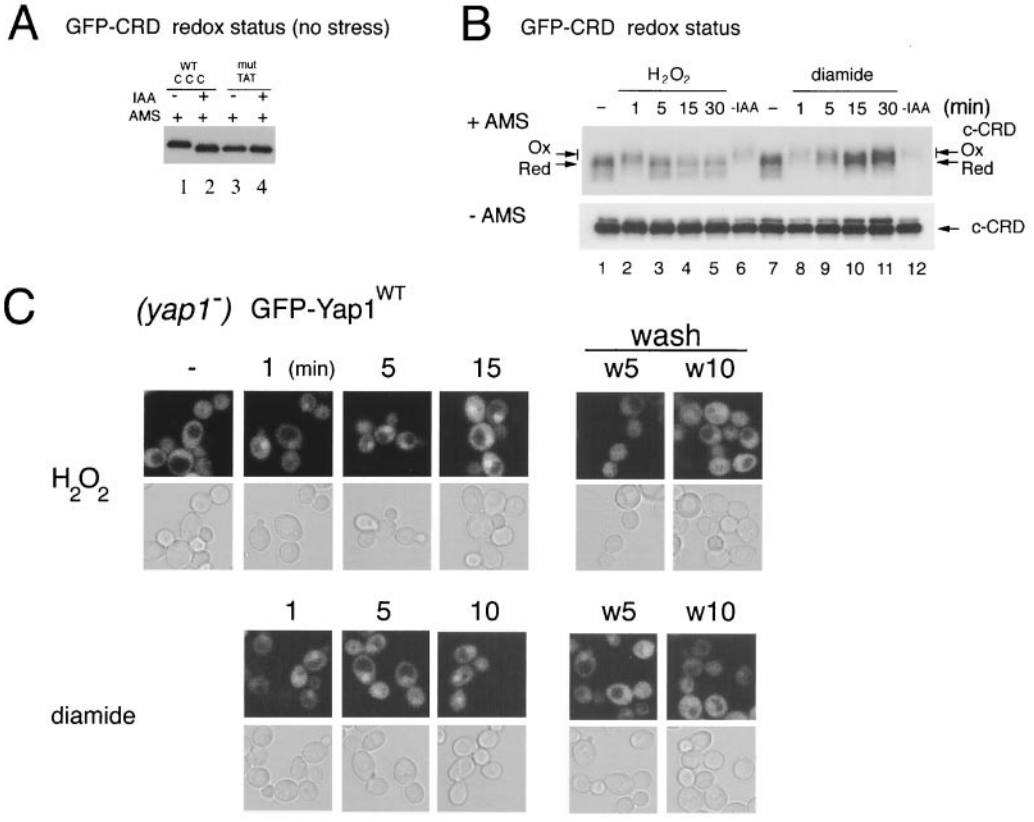

FIG. 3. Correlation between oxidation of c-CRD in vivo and the nuclear localization of Yap1p. (A) The cysteine residues in the c-CRD are reduced in vivo under unstressed conditions. TW (*yap1*) cells carrying pRS HA GFP-c-CRD (lanes 1 and 2) or pRS HA GFP-c-CRD$^{(TAT)}$ (lanes 3 and 4) were cultured until exponential phase and were analyzed for free and oxidized thiols using AMS (with or without pretreatment with IAA) as described in Materials and Methods. Eight-centimeter SDS-PAGE gels were used. (B) Time-dependent oxidation of cysteine residues in the c-CRD in response to H_2O_2 (0.5 mM) or diamide (1.5 mM). Free and oxidized thiols were analyzed as described for panel A at the indicated times (min) after imposition of oxidative stress or without stress (−; lanes 1 and 7). Thirteen-centimeter SDS-PAGE gels were used. Arrows, migration of the reduced (Red) and oxidized (Ox) forms after AMS treatment. (C) Time-dependent nuclear accumulation of Yap1p in response to H_2O_2 or diamide. TW (*yap1*) cells carrying pRS-HA-GFP-YAP1 were cultured until exponential phase, collected, and resuspended in medium containing 0.5 mM H_2O_2 or 1.5 mM diamide. GFP fluorescence was observed by confocal microscopy before oxidant treatment (−) and after the indicated times of treatment (min). After 15 min of oxidant treatment, cells were collected, washed, and resuspended in the same medium without oxidants, and the GFP fluorescence was observed 5 (w5) and 10 (w10) min later.

+AMS). However, a portion of the c-CRD migrated to the fully oxidized position after treatment with diamide for 30 min (Fig. 3B, compare lanes 8 and 6 or 12 of +AMS). It should be noted that the band present at the diamide treatment 1-min time point was decreased in apparent abundance (Fig. 3B, lanes 8; compare +AMS and −AMS). We speculate that mixed disulfide linkage of the c-CRD with cellular proteins might be formed during in vitro treatment of AMS in samples in which the level of free thiols is expected to be high, such as the control samples that were not fixed by IAA (Fig. 3B, lanes 6 and 12).

To test if this oxidation process was correlated with the induced nuclear localization of full-length Yap1p, we observed time dependence of the diamide-induced and H_2O_2-induced nuclear accumulation of GFP-Yap1p. As shown in Fig. 3C, when cells were treated with 0.5 mM H_2O_2, nuclear accumulation of Yap1p was initiated within 1 min (that is, when the c-CRD started to oxidize, see above), and its accumulation at maximal level was completed within 5 min. Similarly, diamide-induced Yap1p nuclear localization started within 1 min (Fig. 3C). These results clearly indicated that the oxidative stress-induced nuclear localization of Yap1p is correlated with the induced oxidation of the cysteine residues in the c-CRD.

We next examined restoration of Yap1p localization when cells were released from the stresses. After treatment with 0.5 mM H_2O_2 or 1.5 mM diamide for 15 min, the cells were washed and incubated in the same medium without stress. Most of the Yap1p accumulated in the nucleus was diffused to the cytoplasm within 5 min and relocalization was complete by 10 min (Fig. 3C).

Requirement of cysteine residues in n-CRD for prolonged nuclear localization. In the H_2O_2-induced response the oxidized c-CRD in vivo was subsequently reduced after 5 min of incubation, but Yap1p remained in the nucleus (see above). We therefore suspected that n-CRD, which was lacking in the context of HA-GFP-c-CRD protein (Fig. 1A), could affect the response. In fact, it has been suggested that the n-CRD can direct nuclear localization of Yap1p (6, 7). As shown in Fig. 4A, when all 3 cysteine residues in the n-CRD (Cys^{303}, Cys^{310}, and Cys^{315}) (Fig. 1A) were mutated to threonine (GFP-Yap1p^{3Cys}), the *trx-lacZ* reporter gene activation was slightly decreased in response to diamide; however, it was almost com-

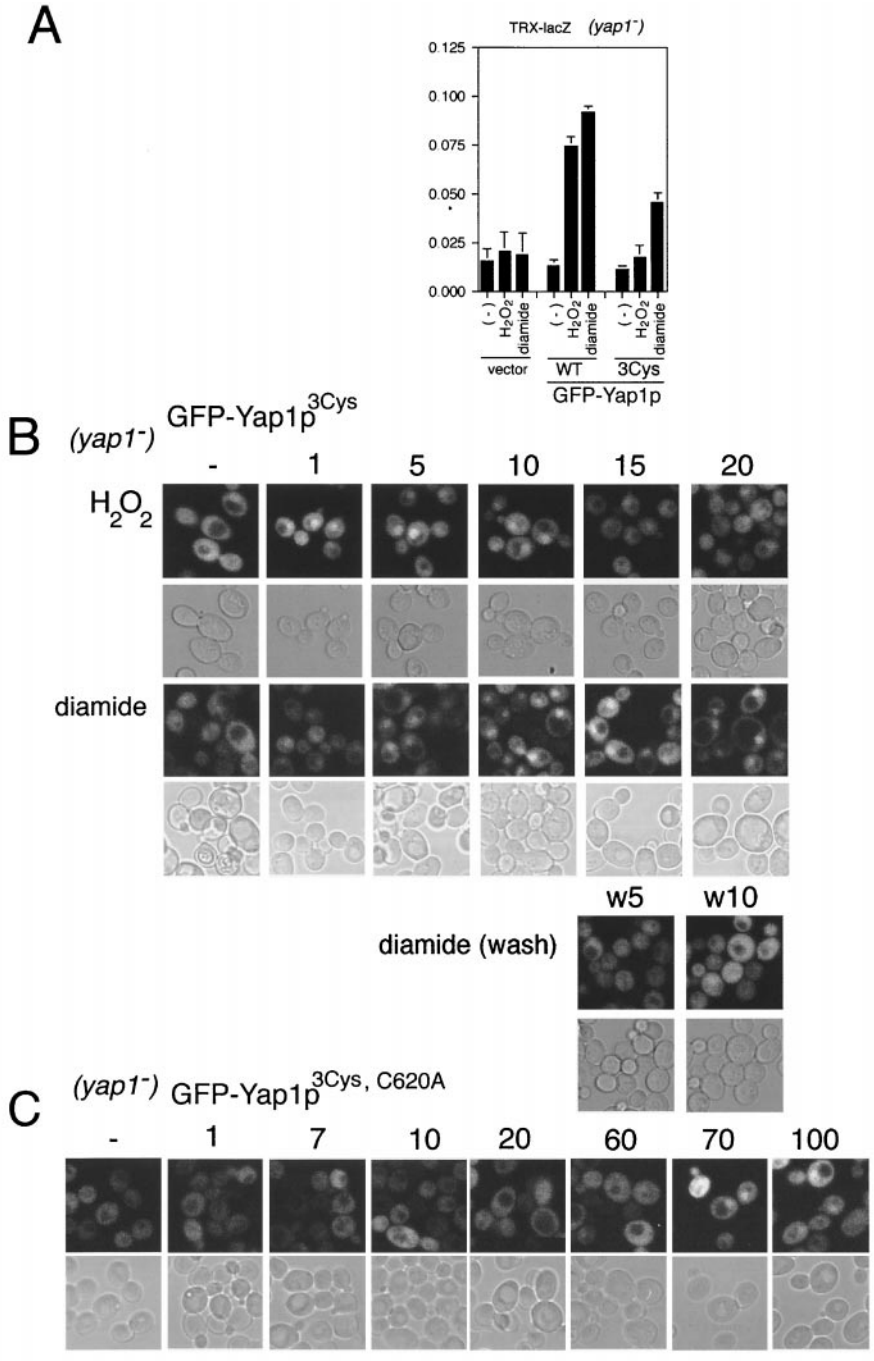

FIG. 4. Requirement of cysteine residues in n-CRD of Yap1p for the prolonged nuclear localization following H_2O_2 treatment but not diamide treatment. (A) The reporter gene (*trx2-lacZ*) activation by Yap1p^{3Cys} was observed as described in the legend to Fig. 2. (B) Time-dependent localization of GFP-Yap1^{3Cys}. Strain TW (*yap1*) expressing GFP-Yap1^{3Cys} was treated with 0.5 mM H_2O_2 or 1.5 mM diamide, and GFP fluorescence was observed before oxidant treatment (−) and at the indicated time of treatment (min) as described in the legend to Fig. 3. The diamide treatment and the release from the stress were carried out as described in the legend to Fig. 3. (C) Time-dependent localization of GFP-Yap1p$^{3Cys,\ C620A}$ in response to 0.5 mM H_2O_2 was observed as described above.

pletely suppressed in response to H_2O_2 (Fig. 4A). Next we observed the time dependence of the H_2O_2-induced nuclear localization (Fig. 4B). As seen for Yap1p^{wt}, H_2O_2 could induce nuclear localization of Yap1p^{3Cys} within 1 min. Interestingly, however, it diffused to cytoplasm within 15 min despite the continual presence of H_2O_2 stress. In contrast, diamide-induced nuclear localization of Yap1p^{3Cys} was similar to that of Yap1p^{wt} (Fig. 3C). That is, nuclear localization was induced within 1 min and persisted. Moreover, when the cells were released from the stress, Yap1p^{3Cys} diffused into the cytoplasm within 5 min. In addition, Yap1p^{3Cys} was localized to the nucleus in *trx1*Δ *trx2*Δ cells (data not shown), suggesting that the

cysteine residues in the n-CRD are not required for nuclear localization under the constitutive oxidizing state. We next address the importance of Cys^{620} by mutating the residue in the $Yap1p^{3Cys}$ mutant. As shown in Fig. 4C, no nuclear localization of $Yap1p^{3Cys,\ C620A}$ in response to H_2O_2 was observed up to 60 min after inhibition of oxidative stress, indicating that Cys^{620} is required for the transient nuclear localization in the context of $Yap1p^{3Cys}$ (see above). Interestingly, nuclear localization of $Yap1p^{3Cys,\ C620A}$ was observed from 70 min after the H_2O_2 treatment, suggesting that this Yap1p mutant has lower sensitivity to H_2O_2.

Cellular redox status of thioredoxin and glutathione in response to oxidative stress. One possible mechanism for oxidation of the cysteine residues in the c-CRD is indirect: change of cellular redox status by the oxidants might trigger formation of a disulfide bond in the c-CRD. Thioredoxin is a crucial factor in the repression of Yap1p nuclear localization (13); moreover, it has recently been shown that Yap1p is constitutively activated in a mutant deficient for thioredoxin reductase (*trr1*) (4; S. Izawa and Y. Inoue, unpublished observation). In such a mutant, the majority of Trx would be in oxidized form. We therefore speculated that the addition of H_2O_2 or diamide might first lead to oxidation of Trx, which would then cause formation of disulfide linkage in the c-CRD. Therefore, we evaluated how the thiol-disulfide ratio (redox status) of thioredoxin was affected by oxidative stress induced by H_2O_2 or diamide. The same samples used for Fig. 3B were separated in SDS-PAGE and were Western blotted with anti-Trx2p-antibody, which recognizes both Trx1p and Trx2p (13). As shown in Fig. 5A, thioredoxin remained reduced for 1 min after addition of H_2O_2 (Fig. 5A, lanes 1 and 2). Oxidized thioredoxin appeared at 5 min and increased to about half of the total amount by 30 min (Fig. 5A, lanes 3 to 5). It is notable that by the time that thioredoxin started to be oxidized (5 min), the c-CRD that had been oxidized at the 1-min time point was decreasing (compare Fig. 3B, lane 3 of +AMS, and Fig. 5A, lane 3). In contrast, 1.5 mM diamide did not affect the thioredoxin redox status (Fig. 3B, lanes 7 to 11). These data clearly indicate that at the time when the c-CRD was oxidized by H_2O_2 and diamide, the thioredoxin was still reduced.

Next we addressed the question of whether c-CRD oxidation in response to oxidative stress by H_2O_2 or diamide occurs via change of glutathione redox status. It has been shown that the ratio of reduced to oxidized glutathione (GSH/GSSG) is not affected after a 1-h treatment with 0.2 mM H_2O_2 (12). We tested the effect of abrupt oxidative stresses on glutathione redox status. As shown in Fig. 5B, the GSH^2/GSSG ratio did not change at any time from 3 to 22 min following the addition of 0.5 mM H_2O_2 (Fig. 5B), indicating that the change of glutathione redox status is unlikely to be responsible for the H_2O_2-induced oxidation of c-CRD. In contrast, diamide did affect the redox status of glutathione: within 7 min of treatment with 1.5 mM diamide, the GSH^2/GSSG ratio fell off to one-third of the ratio under normal conditions (Fig. 5C). When a lower concentration of diamide (0.5 mM) was used, the slope decreased (Fig. 5C). We next measured the GSH^2/GSSG ratio during recovery from the stress. Twelve minutes after the addition of diamide, the cells were washed and resuspended in the same medium lacking diamide and the GSH^2/GSSG ratio was observed. As shown in Fig. 5D, we did not see an increase

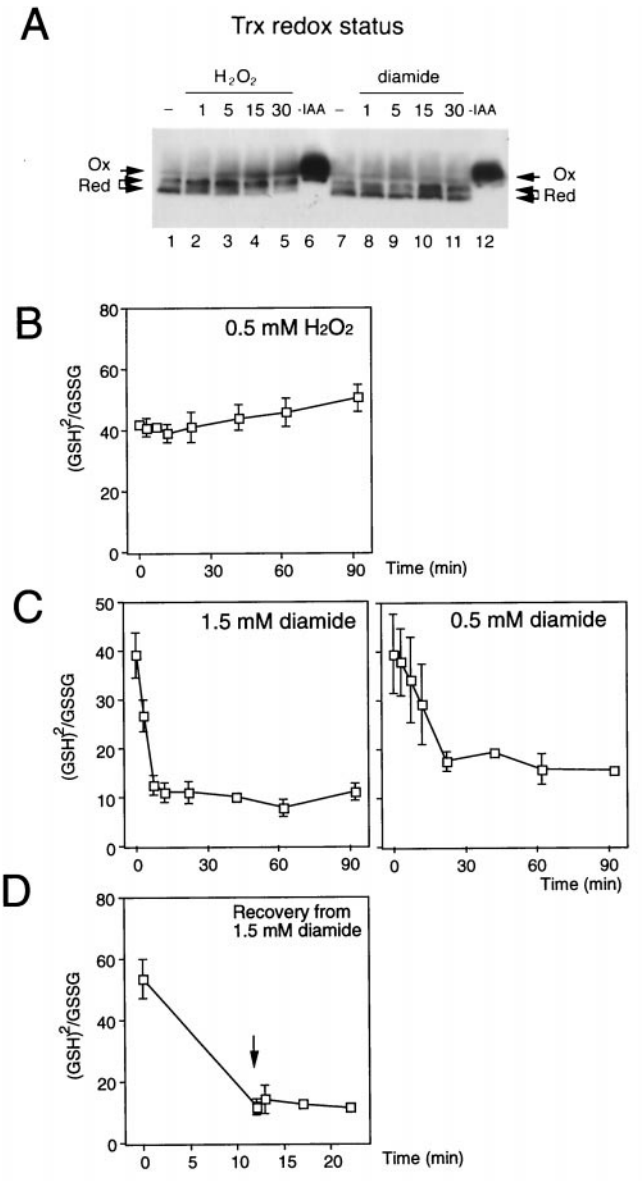

FIG. 5. Redox status of thioredoxin and glutathione. (A) Detection of time-dependent oxidation of thioredoxin in response to H_2O_2 (0.5 mM) or diamide (1.5 mM). The same yeast lysates analyzed for free and oxidized thiols in the experiments for Fig. 3B were separated by SDS–16.5% Tris-Tricine PAGE (26), and thioredoxin (Trx1p and Trx2p) was detected by Western blotting analysis using anti-Trx2p antibody as described in Materials and Methods. Controls for the fully oxidized position were prepared as described in the legend to Fig. 3. Arrows indicate corresponding positions of oxidized (Ox) and reduced (Red) c-CRD. The position of the middle band perhaps corresponds to Trx, of which 1 cysteine reacted with 1 AMS. The yeast Trx proteins have only 2 cysteine residues in their active center which form a disulfide bond in their oxidized form. Thus, at least the middle band is unlikely to be the oxidized form. (B to D) Glutathione redox status in response to oxidative stress. GSH and GSSG were observed in strain TY (*YAP1*) at the times of 0, 3, 7, 12, 22, 42, 62, and 92 min after addition of 0.5 mM H_2O_2 (B) and 1.5 or 0.5 mM diamide (C) as described in Materials and Methods. The redox status of glutathione is indicated as the ratio of GSH^2 to GSSG. (D) Strain TY (*YAP1*) cultured in SD dropout medium was treated with 1.5 mM diamide for 12 min, washed with 0.85% NaCl, and resuspended in the same medium. After 3, 7, and 12 min following the release from oxidative stress, GSH and GSSG were observed. The arrow indicates the time of release from the oxidative stress.

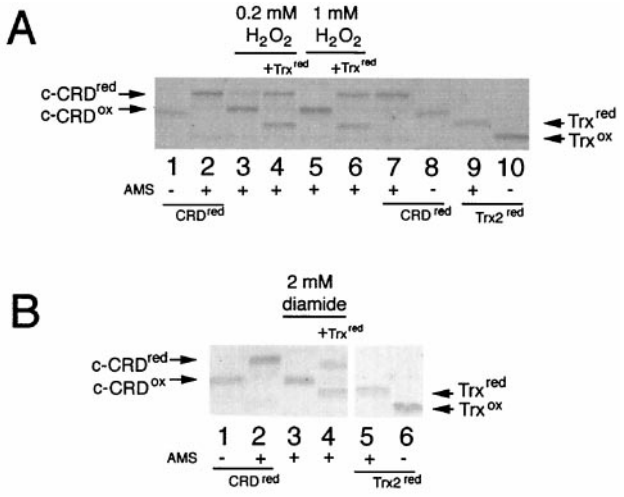

FIG. 6. Reduction of in vitro-oxidized c-CRD by Trx2p. (A) Purified and reduced ΔGFP-CRD was treated with 0.2 mM (lanes 3 and 4) or 1.0 mM (lanes 5 and 6) H_2O_2 and was mixed without (lanes 3 and 5) or with (lanes 4 and 6) reduced Trx2p. SDS–15% PAGE was performed after the reaction with AMS (lanes 2 to 7 and 9) or was not performed (lanes 1, 8, and 10). Controls for the fully reduced ΔGFP-CRD (lanes 2 and 7) and Trx2 (lane 9) were performed by AMS treatment of reduced ΔGFP-CRD and Trx2, respectively, and the samples without AMS treatment were separated as the controls for fully oxidized ΔGFP-CRD (lanes 1 and 8) and thioredoxin (lane 10). (B) The ΔGFP-CRD oxidized with 2 mM diamide (lanes 3 and 4) was reduced by reduced thioredoxin (lane 4). The control for the reduced ΔGFP-CRD (lane 2), the oxidized ΔGFP-CRD (lane 1), reduced thioredoxin (lane 5), and oxidized thioredoxin (lane 6) was created as described above. Arrows indicate the positions of the reduced ΔGFP-CRD (CRD^{red}), oxidized ΔGFP-CRD (c-CRD^{ox}), reduced thioredoxin (Trx^{red}), and oxidized Trx (Trx^{ox}).

in the GSH^2/GSSG ratio within 20 min after the recovery (Fig. 5D). As described above, Yap1p nuclear localization was decreased within 5 to 10 min after release from the stress. Thus, it is unlikely that redox sensing by the c-CRD is mediated by changes in the glutathione redox status affected by diamide.

Reduction of oxidized c-CRD by thioredoxin in vitro. Our results indicate that thioredoxin may be responsible for the rapid reduction of c-CRD as well as recovery of nuclear export after release from oxidative stress. We therefore tested whether thioredoxin could reduce oxidized c-CRD in vitro using the AMS assay and recombinant c-CRD. In this case, AMS was directly reacted with the c-CRD and free thiols were detected by the change in molecular weight. As shown in Fig. 6A, we could detect a clear difference in molecular weight between fully oxidized c-CRD (Fig. 6A, no AMS, lanes 1 and 8) and fully reduced c-CRD (Fig. 6A, with AMS, lanes 2 and 7). When the reduced c-CRD was treated with 0.2 mM (Fig. 6A, lane 3) or 1 mM H_2O_2 (Fig. 6A, lane 5), the cysteine residues were apparently oxidized, since c-CRD migrated faster. However, the H_2O_2-oxidized c-CRD migrated slightly more slowly than the c-CRD not treated with AMS, which corresponded to the fully oxidized form of the c-CRD (Fig. 6A, compare lane 3 or 5 and lane 1 or 8). Perhaps one of the cysteine residues (possibly Cys^{629}, see above) remains reduced under H_2O_2. By the addition of reduced Trx2p, the oxidized c-CRD was converted to a form with the same mobility as reduced c-CRD (Fig. 6A, compare lane 4 or 6 and lane 2 or 7).

We next tested the effect of diamide. As shown in Fig. 6B, diamide could also oxidize the c-CRD (Fig. 6B, lane 3), but in this case, all three cysteine thiols seemed to be oxidized, because the diamide-oxidized c-CRD migrated in the same manner as the fully oxidized c-CRD control (Fig. 6B, compare lanes 1 and 3). Trx2p could also reduce the diamide-oxidized c-CRD (Fig. 6B, lane 4); however, this reduction was partial because the mobility was different from that of fully reduced c-CRD control (Fig. 6B, lane 2). This suggested that diamide could oxidize the 3rd cysteine of c-CRD. Such oxidation may be a sulfenylhydrazine (16). Nevertheless, our results clearly indicated that thioredoxin could reduce H_2O_2-induced and diamide-induced disulfide linkage in the c-CRD.

DISCUSSION

Previous studies indicate that Yap1p is constitutively imported into the nucleus (11); however, continuous nuclear export mediated by Crm1p maintains a relatively low level of Yap1p in the nucleus (19, 32). In response to oxidants like a hydrogen peroxide H_2O_2 or a thiol oxidant diamide, the Crm1p nuclear export step is inhibited. It has been tempting to speculate that the reversible oxidation of thiol residues of cysteines is responsible for regulating the function of the Yap1p c-CRD, because the cysteine residues in the c-CRD are essential for the proper mode of regulation (18) and because interaction of Yap1p with Crm1p is sensitive to oxidative stress both in vivo (19, 32) and in vitro (32).

Here we show that oxidation of cysteine residues of the c-CRD in vivo occurs in accordance with the induced nuclear localization. Under normal growth conditions, most cysteine residues in the c-CRD are not oxidized; however, they become oxidized within 1 min after treatment with H_2O_2 or diamide, at which time Yap1p started to accumulate in the nucleus. Therefore, Yap1p CRD has two forms: a reduced form that has NES function and thus binds to Crm1p (Yap1p is mainly cytoplasm and inactive) and an oxidized form for which the NES function is suppressed, thus releasing Crm1 (Yap1p is localized in the nucleus and active).

Yap1p as possible sensor of H_2O_2 and diamide. Our results indicate that both H_2O_2 and diamide affect cellular redox status, although there is an obvious difference in the cellular responses to the different oxidants. The imposition of H_2O_2 increases the amount of oxidized thioredoxin, but it does not affect the redox status of glutathione (GSH^2/GSSG). This thioredoxin oxidation is most likely coupled to reduction of H_2O_2 via thioredoxin peroxidase (Tsa1p) (5, 24). In contrast, however, diamide has an apparently opposite effect. That is, diamide decreases the GSH^2/GSSG ratio but has no effect on thioredoxin. Diamide can penetrate cell membranes within seconds and react in the cell within minutes (16). Thus, direct oxidation may be carried out to reduce the GSH level inside the cells. Unexpectedly, diamide did not affect redox status of thioredoxin. The GSH and thioredoxin redox buffer systems apparently function as cellular defense systems to cope with oxidative stresses, but their redox status is not directly responsible for activation of Yap1p. Nuclear accumulation of Yap1p and the oxidation of its c-CRD started to occur within the first minute, while the redox status of thioredoxin and glutathione was not affected at the time. Furthermore, the recovery from

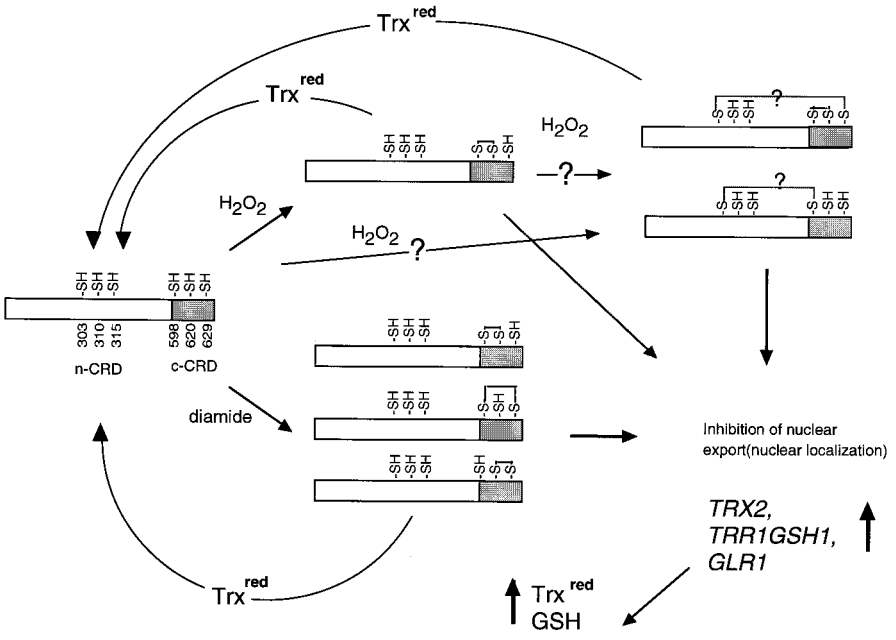

FIG. 7. Models for redox regulation of Yap1p CRD. H_2O_2 or diamide induces disulfide bond formation, leading to dissociation of the c-CRD-Crm1p interaction and consequent nuclear accumulation of Yap1p. Nuclear localized Yap1p results in transcriptional activation of the target genes, such as *TRX2*, which encodes thioredoxin (17, 21); *TRR1*, which encodes thioredoxin reductase (21); *GSH1*, which encodes γ-glutamylcysteine synthetase (31); and *GLR1*, which encodes glutathione reductase (9, 23). Increased expression of *GSH1* and *GLR1* will elevate the GSH level, while increased expression of *TRX2* and *TRR1* will elevate reduced thioredoxin (Trx^{red}) levels. The Yap1p disulfide bonds can be reduced by thioredoxin.

diamide stress rapidly restored the normal subcellular distribution of Yap1p even though GSH^2/GSSG remained. Thus, we presume that the c-CRD can receive (sense) a redox signal directly from the oxidants, leading to nuclear localization of Yap1p and the activation of specific genes for coping with the changing redox status as well as the resulting damages.

Oxidant-specific disulfide bond formation in c-CRD. The processes of disulfide bond formation of the c-CRD were studied using the two different oxidants H_2O_2, and diamide, both of which are apparently good inducers of Yap1p nuclear localization as well as its transcriptional activity (Fig. 2A and 3C) (6,18). Consistent with our previous results that Gal4db-GFP-c-CRD can respond to diamide, the cysteine residues in the c-CRD are responsible for the diamide response. The cysteine residues in the n-CRD seem not to be essential for induced nuclear localization of Yap1p in response to diamide (Fig. 4). There are 3 cysteine residues in the c-CRD (Fig. 1), and the nuclear localization of the c-CRD mutant ($Yap1p^{C598T}$, $Yap1p^{C620A}$, or $Yap1p^{C629T}$) in response to diamide suggests that disulfide linkage between Cys^{598} and Cys^{620}, $Cys^{620}$and Cys^{629}, and Cys^{598} and Cys^{629} can occur. Such disulfide linkage inhibits the interaction of the c-CRD with Crm1p in vivo. It should be noted that the level of the reporter β-galactosidase activity induced by $Yap1p^{3Cys}$ is approximately half that of Yap1p (Fig. 4A), suggesting that the cysteine residues in the n-CRD may function for the constitutive nuclear localization of Yap1p during exposure to oxidants or that the n-CRD cysteine residues may be required for the maximum level of transcription.

The oxidation process by H_2O_2 appears to be more complex. Our results indicate that Cys^{598} and Cys^{629} are essential for the response to H_2O_2. In addition, only $Yap1p^{C598T}$ (among cysteine mutants of Yap1p) is not affected under the oxidizing state of thioredoxin deficiency. Thus, Cys^{598} in the c-CRD appears to be the most crucial residue for sensing H_2O_2. Furthermore, these results indicate that oxidation of cysteines in the c-CRD is sufficient to inhibit Crm1p interaction. In addition, the fact that the disulfide linkage between Cys^{598} and Cys^{620} was specifically induced in vitro indicates that this disulfide linkage may be the initial oxidation of Yap1p. However, H_2O_2-induced nuclear localization of $Yap1p^{3Cys}$ diminishes after 10 min without release from the oxidant treatment, and the protein becomes finally cytoplasmic after 15 min (Fig. 4B). This is consistent with the result of rapid reduction of the c-CRD in vivo in the context of GFP-c-CRD fusion (Fig. 3B). These results suggest an additional mode of regulation is necessary for prolonged nuclear localization. The rapidly induced disulfide linkage may lead to subsequent disulfide formation between a cysteine residue in the n-CRD and Cys^{629} or Cys^{598} (Fig. 7). Although Cys^{620} is apparently essential for rapid response to H_2O_2 in the context $Yap1p^{3Cys,\ C620A}$ (Fig. 4C), induction of nuclear localization of $Yap1p^{C620A}$ is not significantly different from that of Yap1p (data not shown), although the level of the reporter β-galactosidase activity is reduced (Fig. 2A). Thus, another possibility is that direct disulfide linkage between the n-CRD and c-CRD occurs in response to H_2O_2. The possible disulfide linkage between Cys^{303} and Cys^{598}, which shows faster mobility on SDS-PAGE, seems not to be sufficient to inhibit Yap1p-Crm1p interaction (7), suggesting that multiple oxidation events are required for the response. More precise analyses of $Yap1p^{WT}$ using MS are required to understand the interaction of all 6 cysteine residues of Yap1p.

Reversible disulfide bond formation in c-CRD governs its NES activity. Release from oxidative stress results in rapid cytoplasmic relocalization of Yap1p, indicating that a rapid reduction system(s) is coupled with the determination of Yap1p nuclear localization. We show that thioredoxin can reduce oxidized c-CRD in vitro. The finding that $Yap1p^{WT}$ localizes to the nucleus in *trx1*Δ *trx2*Δ mutant cells (13; Fig. 2B) implies that thioredoxin has a potential to reduce cysteine residues of Yap1p in vivo.

In summary, we propose that Yap1p can sense oxidants through reversible disulfide bond formation in the cysteine residues of its c-CRD. Because we see oxidation of thioredoxin at 5 min following the treatment with H_2O_2 and infer that the oxidation state inside the cell may be changed at this time. However, the c-CRD was oxidized more rapidly than thioredoxin and in fact had become reduced again by the 5-min time point, at least in the context of the c-CRD alone. We suspect, therefore, that a transient redox signal of H_2O_2 may be converted to a stabler signal. For example, an oxidized form of Yap1p with a lower redox potential may be required in order to prolong Yap1p nuclear localization until the cellular oxidation status is fully recovered. Our data show that Yap1p can sense redox signal rather than oxidative stress, if the stress is defined as a change of redox status inside the cells.

ACKNOWLEDGMENTS

We thank Gigi Storz (National Institutes of Health, Bethesda, Md.) for her valuable advice and guidance in preparing the manuscript. We thank Masato Kobori and Ryuta Mizutani (Graduate School of Pharmaceutical Sciences, The University of Tokyo) for technical assistance with the MALDI-TOF (MS), the Human Genome Center of IMSUT for computer system as well as Internet service, and Gigi Storz and Orna Carmel-Harel for exchanging unpublished information.

This work was supported by Grants-in-Aid for Scientific Research (C) from the Ministry of Education, Science, Sports and Culture of Japan.

REFERENCES

1. **Anderson, M. E., and A. Meister.** 1985. Preparation of γ-glutamyl amino acids by chemical and enzymatic methods. Methods Enzymol. **113:**555–564.
2. **Aslund, F., M. Zheng, J. Beckwith, and G. Storz.** 1999. Regulation of the OxyR transcription factor by hydrogen peroxide and the cellular thiol-disulfide status. Proc. Natl. Acad. Sci. USA **96:**6161–6165.
3. **Carmel-Harel, O., and G. Storz.** 2000. Role of the glutathione- and thioredoxin-dependent reduction system in the *Escherichia coli* and *Saccharomyces cerevisiae* response to oxidative stress. Annu. Rev. Microbiol. **54:**439–461.
4. **Carmel-Harel, O., R. Stearman, A. P. Gasch, D. Botstein, P. O. Brown, and G. Storz.** 2001. Role of thioredoxin reductase in the Yap1p-dependent response to oxidative stress in *Saccharomyces cerevisiae*. Mol. Microbiol. **39:**595–605.
5. **Chae, H. Z., S. J. Chung, and S. G. Rhee.** 1994. Thioredoxin-dependent peroxide reductase from yeast. J. Biol. Chem. **269:**27670–27678.
6. **Coleman, S. T., E. A. Epping, S. M. Steggerda, and W. S. Moye-Rowley.** 1999. Yap1p activates gene transcription in an oxidant-specific fashion. Mol. Cell. Biol. **19:**8302–8313.
7. **Delaunay, A., A. D. Isnard, and M. B. Toledano.** 2000. H_2O_2 sensing through oxidation of the Yap1 transcription factor. EMBO J. **19:**5157–5166.
8. **Dunn, B., and C. R. Wobbe.** 1997. *Saccharomyces cerevisiae*, p. 13.1.2–13.1.3. *In* R. Ausubel, R. Brent, and R. E. Kingston (ed.), Current protocols in molecular biology. John Wiley & Sons, Inc., New York, N.Y.
9. **Grant, C. M., L. P. Collinson, J. H. Roe, and I. W. Dawes.** 1996. Yeast glutathione reductase is required for protection against oxidative stress and is a target gene for yAP-1 transcriptional regulation. Mol. Microbiol. **21:**171–179.
10. **Halliwell, B., and J. M. C. Gutteridge.** 1999. Free radicals in biology and medicine. Oxford Science Publications, Oxford, England.
11. **Isoyama, T., A. Murayama, A. Nomoto, and S. Kuge.** 2001. Nuclear import of the yeast AP-1 like transcription factor Yap1p is mediated by import receptor Pse1p, and this import step is not affected by oxidative stress. J. Biol. Chem. **276:**21863–21869.
12. **Izawa, S., K. Maeda, T. Miki, J. Mano, Y. Inoue, and A. Kimura.** 1998. Importance of glucose-6-phosphate dehydrogenase in the adaptive response to hydrogen peroxide in *Saccharomyces cerevisiae*. Biochem. J. **330:**811–817.
13. **Izawa, S., K. Maeda, K. Sugiyama, J. Mano, Y. Inoue, and A. Kimura.** 1999. Thioredoxin deficiency causes the constitutive activation of Yap1, an AP-1-like transcription factor in *Saccharomyces cerevisiae*. J. Biol. Chem. **274:**28459–28465.
14. **Jakob, U., W. Muse, M. Eser, and J. C. Bardwell.** 1999. Chaperone activity with a redox switch. Cell **96:**341–352.
15. **Jamieson, D. J.** 1998. Oxidative stress responses of the yeast *Saccharomyces cerevisiae*. Yeast **14:**1511–1527.
16. **Kosower, N. S., and E. M. Kosower.** 1995. Diamide: an oxidant probe for thiols. Methods Enzymol. **251:**123–133.
17. **Kuge, S., and N. Jones.** 1994. *YAP1* dependent activation of *TRX2* is essential for the response of *Saccharomyces cerevisiae* to oxidative stress by hydroperoxides. EMBO J. **13:**655–664.
18. **Kuge, S., N. Jones, and A. Nomoto.** 1997. Regulation of yAP-1 nuclear localization in response to oxidative stress. EMBO J. **16:**1710–1720.
19. **Kuge, S., T. Toda, N. Iizuka, and A. Nomoto.** 1998. Crm1 (XpoI) dependent nuclear export of the budding yeast transcription factor yAP-1 is sensitive to oxidative stress. Genes Cells **3:**521–532.
20. **Meister, A., and M. F. Anderson.** 1983. Glutathione. Annu. Rev. Biochem. **52:**711–760.
21. **Morgan, B. A., G. R. Banks, W. N. Toone, D. Raitt, S. Kuge, and L. H. Johnston.** 1997. The Skn7 response regulator controls gene expression in the oxidative stress response of the budding yeast *Saccharomyces cerevisiae*. EMBO J. **16:**1035–1044.
22. **Moye-Rowley, W. S., K. D. Harshman, and C. S. Parker.** 1989. Yeast *YAP1* encodes a novel form of the jun family of transcriptional activator proteins. Genes Dev. **3:**283–292.
23. **Muller, E. G.** 1996. A glutathione reductase mutant of yeast accumulates high levels of oxidized glutathione and requires thioredoxin for growth. Mol. Biol. Cell **7:**1805–1813.
24. **Ross, S. J., V. J. Findlay, P. Malakasi, and B. A. Morgan.** 2000. Thioredoxin peroxidase is required for the transcriptional response to oxidative stress in budding yeast. Mol. Biol. Cell **11:**2631–2642.
25. **Sambrook, J., E. F. Fritsch, and T. Maniatis.** 1989. Molecular cloning: a laboratory manual, 2nd ed. Cold Spring Harbor Laboratory Press, Cold Spring Harbor, N.Y.
26. **Schägger, H., and G. von Jagow.** 1987. Tricine-sodium dodecyl sulfate-polyacrylamide gel electrophoresis for the separation of proteins in the range from 1 to 100 kDa. Anal. Biochem. **166:**368–379.
27. **Shiroki, K., T. Isoyama, S. Kuge, T. Ishii, S. Ohmi, S. Hata, K. Suzuki, Y. Takasaki, and A. Nomoto.** 1999. Intracellular redistribution of truncated La protein produced by poliovirus 3Cpro-mediated cleavage. J. Virol. **73:**2193–2200.
28. **Spector, A., G. Z. Yan, R. R. Huang, M. J. McDermott, P. R. Gascoyne, and V. Pigiet.** 1988. The effect of H_2O_2 upon thioredoxin-enriched lens epithelial cells. J. Biol. Chem. **263:**4984–4990.
29. **Toone, W. M., and N. Jones.** 1998. Stress-activated signaling pathways in yeast. Genes Cells **3:**485–498.
30. **Wemmie, J. A., M. S. Szczypka, D. J. Thiele, and W. S. Moye-Rowley.** 1994. Cadmium tolerance mediated by the yeast AP-1 protein requires the presence of an ATP-binding cassette transporter-encoding gene, *YCF1*. J. Biol. Chem. **269:**32592–32597.
31. **Wu, A.-L., and W. S. Moye-Rowley.** 1994. *GSH1*, which encodes γ-glutamylcysteine synthetase, is a target gene for yAP-1 transcriptional regulation. Mol. Cell. Biol. **14:**5832–5839.
32. **Yan, C., L. H. Lee, and L. I. Davis.** 1998. Crm1p mediates regulated nuclear export of a yeast AP-1-like transcription factor. EMBO J. **17:**7416–7429.
33. **Zheng, M., F. Aslund, and G. Storz.** 1998. Activation of the OxyR transcription factor by reversible disulfide bond formation. Science **279:**1718–1721.
34. **Zheng, M., and G. Storz.** 2000. Redox sensing by prokaryotic transcription factors. Biochem. Pharmacol. **59:**1–6.